The Journal of Experimental Biology 205, 321–325 (2002)
Printed in Great Britain © The Company of Biologists Limited 2002
JEB3848

Evidence for increased myofibrillar mobility in desmin-null mouse skeletal muscle

Sameer B. Shah[1], Fong-Chin Su[2], Kimberly Jordan[1], Derek J. Milner[3], Jan Fridén[4], Yassemi Capetanaki[3] and Richard L. Lieber[1,]*

[1]*Departments of Orthopaedics and Bioengineering, Veterans Affairs Medical Center and University of California at San Diego, San Diego, CA 92093, USA,* [2]*Institute of Biomedical Engineering, National Cheng Kung University, Tainan, Taiwan,* [3]*Department of Cell Biology, Baylor College of Medicine, Houston, TX 77030, USA* and [4]*Department of Hand Surgery, Sahlgrenska University Hospital, Göteborg, Sweden*

*Author for correspondence (e-mail: rlieber@ucsd.edu)

Accepted 22 November 2001

Summary

Quantitative electron microscopy was used to characterize the longitudinal mobility of myofibrils during muscle extension to investigate the functional roles of skeletal muscle intermediate filaments. Extensor digitorum longus fifth toe muscles from wild-type (+/+) and desmin-null (des –/–) animals were passively stretched to varying lengths, and the horizontal displacement of adjacent Z-disks in neighboring myofibrils (Δx_{myo}) and average sarcomere length (SL) were calculated. At short SL (<2.20 μm), wild-type and desmin-null Δx_{myo} were not significantly different, although there was a trend towards greater Z-disk misalignment in muscles from knockout animals (Δx_{myo} 0.34±0.04 μm *versus* 0.22±0.09 μm; $P>0.2$; means ± S.E.M.). However, at higher SL (>2.90 μm), muscles from knockout animals displayed a dramatically increased Δx_{myo} relative to wild-type muscles (0.49±0.10 μm *versus* 0.25±0.07 μm; $P<0.05$). The results, which establish a maximum extension of the desmin network surrounding the Z-disk, provide what we believe to be the first quantitative estimation of the functional limits of the desmin intermediate filament system in the presence of an intact myofibrillar lattice. The existence of a limit on the extension of desmin suggests a mechanism for the recruitment of desmin into a network of force transmission, whether as a longitudinal load bearer or as a component in a radial force-transmission system.

Key words: passive strain, electron microscopy, intermediate filament, force transmission, muscle, mouse.

Introduction

Desmin, the most abundant intermediate filament protein in adult striated muscle, plays a critical role in the organization of the myofibrillar matrix. Desmin connects Z-disks laterally and, to a lesser extent, longitudinally to one another as well as to nuclei, mitochondria and costameres (Georgatos et al., 1987; Granger and Lazarides, 1979, 1982; Lazarides, 1982; Milner et al., 2000; Richardson et al., 1981; Tokuyasu et al., 1982; Wang and Ramirez-Mitchell, 1983). Because of the extensive co-localization of desmin and these critical elements within the muscle fiber, it is believed that the intermediate filament network plays the mechanical role of maintaining proper alignment of cellular structures during physiological functioning of muscle (Lazarides, 1980; Milner et al., 1996).

In spite of plentiful information regarding the localization of desmin filaments throughout the muscle cell, there is scant evidence for the mechanical function of the intermediate filament system in skeletal muscle. In 'ghost' muscle fibers, in which the myofibrillar apparatus was chemically extracted, Wang and Ramirez-Mitchell (1983) measured significant mechanical load-bearing by intermediate filaments only at very long sarcomere lengths, over 5 μm. This result suggested that the muscle intermediate filaments may not bear significant loads at physiological sarcomere lengths, which rarely exceed 3.5 μm (Burkholder and Lieber, 2001). However, indirect evidence suggests that desmin does play an important functional role in normal muscle. Muscles from desmin-null (des –/–) mice created *via* homologous recombination (Li et al., 1996; Milner et al., 1996) generate a lower isometric stress (Sam et al., 2000) and exhibit decreased strength (Li et al., 1997) than muscles from wild-type (+/+) mice. However, paradoxically, in spite of the 'weakness' of these muscles, the desmin-null muscles appear to be protected from the mechanical injury that occurs after a bout of eccentric contractions, even when corrected for the lower stresses generated by the muscles from knockout animals (Sam et al., 2000). It is difficult to explain such observations on the basis of the immunolocalization and ultrastructural data currently available. Thus, the purpose of the present study was to quantify the longitudinal mobility of myofibrils during muscle extension to elucidate further the functional roles of intermediate filaments in skeletal muscle.

Materials and methods

Experiments were performed on the fifth toe muscle of the extensor digitorum longus (EDL) muscle in two groups of age-matched young adult mice: wild-type 129/Sv (*N*=7, 8–12 weeks; Taconic Farms, Germantown, NY, USA) and desmin homozygous knockout 129/Sv (*N*=9, aged 8–12 weeks) (Milner et al., 1996). The EDL of the fifth toe was chosen on the basis of its distinct origin and insertion tendons, fiber length homogeneity, unipennate architecture and predominantly fast fiber-type distribution (Chleboun et al., 1997). Accordingly, the fifth toe model allows for consistent application of longitudinal passive loads in a system free from the confounding effects of fiber rotation or pre-existing ultrastructural abnormalities, such as those potentially present in chronically activated desmin-null muscles such as the soleus or diaphragm (Li et al., 1996; Milner et al., 1996).

All procedures were performed in accordance with the NIH Guide for the Use and Care of Laboratory Animals and were approved by the University of California and Department of Veteran's Affairs Committees on the Use of Animal Subjects in Research. Each mouse was anesthetized with a cocktail of 10 mg kg^{-1} ketamine, 5 mg kg^{-1} rompum and 1 mg kg^{-1} acepromazine delivered by intraperitoneal injection. The mouse was then killed by intracardiac injection of concentrated sodium pentobarbital. The hindlimbs were skinned and transected below the hip, leaving the entire knee joint intact, and placed for further dissection (within 15 min of death) into a Ringer's solution (adjusted to pH 7.5) composed of 137 mmol l^{-1} NaCl, 5 mmol l^{-1} KCl, 1 mmol l^{-1} NaH_2PO_4, 2 mmol l^{-1} $CaCl_2$, 1 mmol l^{-1} $MgSO_4$ and 11 mmol l^{-1} glucose containing 10 mg l^{-1} curare. Each muscle was then dissected, passively stretched from approximately 100 to approximately 150 % of slack muscle length to generate a range of sarcomere lengths and tied to a wooden applicator.

Stretched muscles were submerged into phosphate-buffered Karnovsky's fixative (6 % buffered glutaraldehyde plus formaldehyde), in which they were allowed to incubate overnight at 4 °C. Specimens were washed three times in cold (4 °C) sodium cacodylate buffer (0.1 mol l^{-1} adjusted to pH 7) and then further fixed in 2 % osmium tetroxide for 1 h at room temperature (23 °C). After three buffer washes of 5 min each, muscles were dehydrated in a graded ethanol series and propylene oxide. Specimens were then cut into approximately equal-sized pieces, embedded in Scipoxy 812 Resin (Energy Beam Sciences, Agawam, MA, USA) and oriented to enable longitudinal sectioning. Micrographs were photographed from longitudinal sections of deep and superficial regions (approximately 150 μm^2 per micrograph) randomly distributed through the fiber (five micrographs for each depth, giving 10 micrographs per muscle). The sections were confirmed to be in perfect longitudinal alignment by tracking the myofibrils (maximum diameter approximately 0.7 μm) across the entire micrograph (maximum length approximately 14 μm) without observing myofibrils shifting into and out of the section plane.

The end points of all Z-disks from each micrograph were digitized (Fig. 1), allowing the quantification of the horizontal displacement of adjacent Z-disks (Δx_{myo}; 45–80 measurements per micrograph) and the calculation of sarcomere length (SL; five measurements per micrograph).

The contributions of myofibrils, sarcoplasmic reticulum and mitochondria to total cell volume were quantified using stereological techniques on each of the longitudinal sections

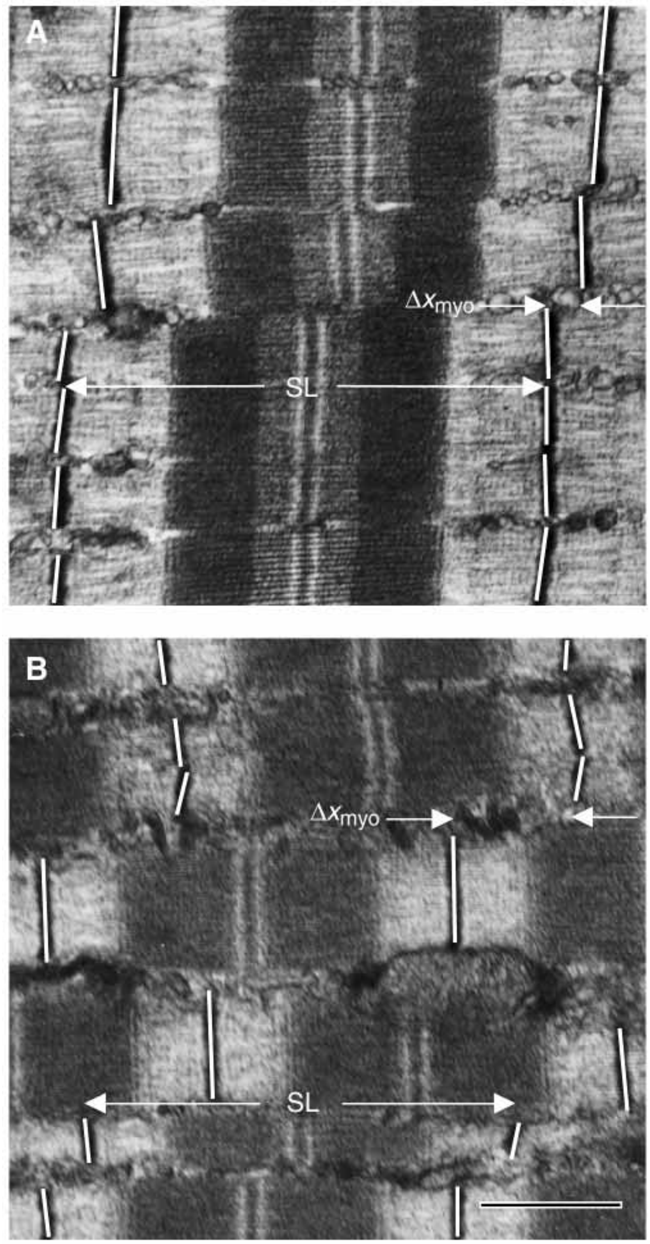

Fig. 1. Electron micrographs of the extensor digitorum longus fifth toe muscle from wild-type (A) or desmin-null (B) animals fixed under conditions of passive loading, displaying the method for digitizing Z-disk endpoints to yield horizontal Z-disk displacement (Δx_{myo}) and sarcomere length (SL). Note the greater stagger in adjacent Z disks in muscle from knockout *versus* wild-type animals. For the frames displayed (approximately one-fifteenth the area of a full micrograph), for (A), Δx_{myo}=0.09 μm and SL=3.57 μm, for (B), Δx_{myo}=0.58 μm and SL=3.60 μm. The calibration is identical for both micrographs. Scale bar, 1 μm.

described above. To prevent pattern recognition or bias during micrograph analysis, sets of micrographs from both superficial and deep regions of muscles from wild-type and desmin-null mice were catalogued and merged in random order. In addition, the technician responsible for analysis did not know the hypothesized results, fiber depth or genotype of the micrographs.

A 10×10 grid of 15 mm squares was printed on a transparency, and coordinates were numbered on each side. The grid was placed at a fixed point on each micrograph, and the structure at each one of the 100 intersecting test points was categorized as myofibril, mitochondria, sarcoplasmic reticulum (SR) or 'other,' where 'other' represented extramyofibrillar structures that could not definitively be categorized as either mitochondria or SR. At test points lying on borders between structures, the component visible in the upper left corner of the intersection was credited to the point in question. Finally, micrographs were resorted into their original groups upon completion of point counting, and the test point fraction of each structure was tabulated, corresponding to the volume density, or volume fraction, of each structure (Weibel, 1980).

An unpaired *t*-test was used to determine whether horizontal Z-disk displacement and/or sarcomere length were significantly different in deep and superficial regions of muscle fibers, and linear regression was used to measure the association between Δx_{myo} and SL in response to passive stretch. The slopes for data from muscles of wild-type *versus* knockout animals were compared by analysis of covariance (ANCOVA). Differences in misalignment at short (SL<2.20 µm) and long (SL>2.90 µm) sarcomere lengths, corresponding to strains resulting in insignificant and significant passive loads, respectively, were compared by one-way analysis of variance (ANOVA) (Statview 5.0, Abacus Concepts, Inc., Berkeley, CA, USA). The range of sarcomere lengths analyzed also corresponds to the shortest and longest operating sarcomere lengths for the mouse EDL (James et al., 1995). Values obtained from point counting were compared using a two-way ANCOVA, with genotype (wild-type *versus* desmin-null) and depth (superficial *versus* deep) as grouping factors and sarcomere length as the covariate.

Results

Horizontal Z-disk displacement, Δx_{myo}, in deep and superficial regions of EDL fifth toe muscles from knockout and wild-type animals was plotted against sarcomere length to characterize myofibrillar mobility with increasing sarcomere strain (Fig. 2). There were no significant differences in Δx_{myo} or SL between superficial and deep regions of muscle fibers within muscles of knockout or wild-type animals (unpaired *t*-test, SL, P=0.95; Δx_{myo}, P=0.92). Consequently, the data were pooled from the superficial and deep regions within each muscle type for further statistical analysis. At short SL (<2.20 µm), wild-type and desmin-null Δx_{myo} values were not significantly different, although there was a trend towards greater Z-disk misalignment in muscles from knockout animals (0.34±0.04 µm *versus* 0.22±0.09 µm, P>0.2; means ± S.E.M.). However, at higher SL (>2.90 µm), muscles from knockout animals displayed an increased Δx_{myo} relative to muscles from wild-type animals (0.49±0.10 µm *versus* 0.25±0.07 µm, P<0.05).

The observation that there is a difference in Δx_{myo} between myofibrils from knockout and wild-type animals with increasing sarcomere strain was supported by the fact that the regression slope of the Δx_{myo} *versus* SL relationship was significantly different from zero in the specimens from knockout animals (P<0.005) but not in specimens from wild-type animals (P>0.4). In addition, ANCOVA revealed a significant difference between the slopes of these relationships (P<0.05). Finally, the coefficients of determination (r^2) and regression slopes (m) were both dramatically higher in the specimens from knockout animals compared with wild-type animals (wild-type, m=0.03, r^2=0.10; knockout, m=0.15, r^2=0.81). Taken together, a significant difference in the Δx_{myo} value between genotypes was seen as a function of sarcomere length in this experiment.

No significant differences in myofibrillar, mitochondrial or SR content between muscles from wild-type or desmin-null

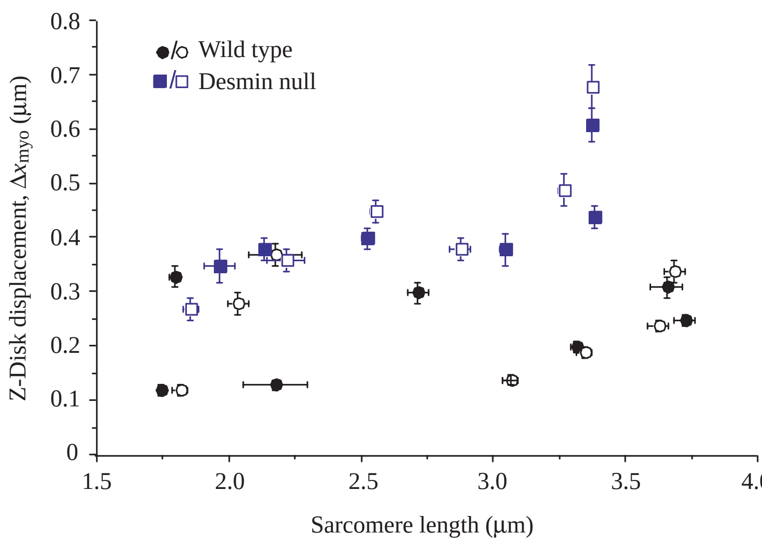

Fig. 2. Horizontal Z-disk displacement (Δx_{myo}) plotted *versus* sarcomere length (SL) for extensor digitorum longus fifth toe muscles of wild-type (circles) and desmin-null (squares) animals. Superficial regions are shown with open symbols while deep regions are shown with filled symbols. Note that Δx_{myo} increases to a greater extent as SL increases in muscles from knockout compared with wild-type animals. Error bars represent ±1 S.E.M. in either the Δx_{myo} or SL direction (N=7 wild-type muscles and N=9 desmin-null muscles). Superficial and deep regions of each muscle were sampled from 10 micrographs per region. The regression slope of the Δx_{myo} *versus* SL relationship was significantly different from zero in the specimens from knockout animals (P<0.005) but not in the specimens from wild-type animals (P>0.4), and analysis of covariance (ANCOVA) revealed a significant difference between the slopes of these relationships (P<0.05).

Table 1. *Volume per cent of structures in muscle samples*

	Wild type		Desmin null	
Structure	Deep (%)	Superficial (%)	Deep (%)	Superficial (%)
Myofibril	78.2±1.7	78.6±1.5	82.9±2.7	76.0±2.1
Mitochondria	4.9±0.7	4.0±0.6	4.3±1.1	5.1±1.2
Sarcoplasmic reticulum	7.9±1.8	9.7±1.7	6.2±1.6	6.5±2.1

Values are means ± S.E.M.; N=10 micrographs per muscle.

No significant differences were observed between genotypes or depths.

animals were observed (P>0.6), nor were differences seen as a function of depth (P>0.6) (Table 1). Sarcomere length was noted to be a significant covariate (P<0.01) from ANCOVA, indicating that these values were sensitive to the fixation length.

Discussion

This study provides what we believe to be the first quantification of the limits of functional extension of the desmin intermediate filament system in the presence of an intact myofibrillar lattice. Inspection of electron micrographs revealed that the sarcomeres themselves, within a single myofibril, are phenotypically normal, exhibiting the characteristic Z-disk, I-band and A-band morphology (Fig. 1). However, the increase in Z-disk misalignment with increasing sarcomere length in muscles from desmin-null specimens suggests that desmin plays a role in organizing intact myofibrils laterally during mechanical loading by tethering adjacent Z-disks. It is also possible that the absence of longitudinal desmin linkages may result in a more random and misaligned myofibrillar network. However, this seems unlikely since it would probably also result in a large sarcomere length variation longitudinally, which was not the case (see horizontal error bars in Fig. 2).

The maximum ‘tethering radius’ (a term coined to describe the maximum longitudinal extension of the desmin network surrounding a Z-disk) is estimated to be approximately 0.32 µm from the Z-disk displacement in muscles from wild-type animals at high passive strain. This value remained relatively constant as a function of sarcomere length. In contrast, in knockout animals, the value of Δx_{myo} increased as a function of sarcomere length and, thus, an upper value for tethering radius cannot be readily inferred (Fig. 2). The existence of a limit on the extension of desmin in wild-type animals suggests a mechanism for the recruitment of desmin into a network of force transmission, whether as a longitudinal load bearer or as a component in a radial force-transmission system. Specifically, desmin could act as a highly compliant or unloaded spring at low extensions, but at increasing extension would exhibit the properties of an extremely stiff spring or, quite possibly, a rigid linkage. Details of this relationship could be elucidated by characterizing the mechanical properties of the desmin filaments themselves. In addition, such a network of filamentous connections, which integrates the entire cytoskeleton, could play an important role in strain-mediated signal transduction, such as that suggested by a study of endothelial cells (Maniotis et al., 1997). Analogous studies could be envisioned in muscle, in which force- and length-transducing mechanisms could be carefully studied in wild-type or desmin-null mice.

The absence of a tethering radius in muscles from knockout animals argues against other intermediate filaments providing a substitute function for absent desmin. These proteins include those associated with the M-line, such as skelemin (Price, 1987; Price and Gomer, 1993). These filaments either have a fracture stress less than the passive stress imposed at high strains, and are therefore damaged during increased extension, or are extremely compliant at high strains, and therefore play a minimal role in the structural organization of myofibrils. Finally, from a design standpoint, the absence of a limit to Δx_{myo} in desmin-null muscles provides further evidence against any upregulation of functionally analogous intermediate filament proteins in the knockout system that would mimic desmin function, such as paranemin, synemin or plectin (Carlsson et al., 2000), since, if these proteins were dramatically upregulated, one might expect less mobility in the myofibrils of muscles from desmin-null animals.

Differences in Z-disk displacement between muscles from wild-type and knockout animals may explain the observation of the lower isometric stress generated by desmin-null muscles as well as their reduced susceptibility to injury that we recently reported (Sam et al., 2000). However, Z-disk displacement was measured in the previous study only from specimens at slack length. Thus, it was not clear whether the differences were permanent, fixed differences between muscles or whether they suggested underlying differences in interconnections between adjacent myofibrils. The present data support the idea of differences in interconnections between muscles of different genotypes. On the basis of the increased mobility observed in desmin-null muscles, sliding of adjacent myofibrils could result in inefficient force transmission due to energy dissipation (explaining the lower isometric stress). Using similar logic, mechanically uncoupling myofibrils during mechanical loading of a muscle fiber could serve a protective role (explaining the decreased muscle injury). It is conceivable that damaged myofibrils without a surrounding desmin intermediate filament lattice (Lieber et al., 1996) would have an opportunity to repair themselves prior to re-integrating themselves into the load-bearing network. During this myofibrillar repair, muscle function would not be completely compromised since other sarcomeres could transmit force normally. It does not appear that the increase in myofibrillar mobility or decrease in force-generating ability (Sam et al., 2000) in muscles from desmin-knockout animals is due to inherent differences in myofibrillar content (Table 1). Note, however, that it is possible that stereology of transverse muscle sections may reveal differences in the density of structures involved in the excitation–contraction coupling process.

Finally, the observation of increased Z-disk mobility in desmin-knockout mice at SL well below 5.0 μm, i.e. lengths at which Wang and Ramirez-Mitchell (1983) reported significant passive load-bearing ability in 'ghost' fibers, suggests that the role of intermediate filaments should be re-examined in a system free from the confounding geometrical effects of sarcomere protein extraction. In particular, it is possible that the collapse of the intermediate filament system as a result of myofibrillar extraction altered the mechanical boundary conditions of the intermediate filament lattice during testing, thereby significantly affecting the mechanical properties measured.

This work was supported by the Department of Veterans Affairs and NIH grant 40050 and the Swedish Medical Research Council. We thank Heather Ross for excellent technical assistance and Professor Odile Mathieu-Costello (UC San Diego) for assistance in designing the stereology protocol.

References

Burkholder, T. J. and Lieber, R. L. (2001). Sarcomere length operating range of muscles during movement. *J. Exp. Biol.* **204**, 1529–1536.

Carlsson, L., Li, Z. L., Paulin, D., Price, M. G., Breckler, J., Robson, G., Wiche, G. and Thornell, L. E. (2000). Differences in the distribution of synemin, paranemin and plectin in skeletal muscles of wild-type and desmin knock-out mice. *Histochem. Cell Biol.* **114**, 39–47.

Chleboun, G. S., Patel, T. J. and Lieber, R. L. (1997). Skeletal muscular architecture and fiber type distribution with the multiple bellies of the mouse extensor digitorum longus muscle. *Acta Anat.* **159**, 147–155.

Georgatos, S. D., Weber, K., Geisler, N. and Blobel, G. (1987). Binding of two desmin derivatives to the plasma membrane and the nuclear envelope of avian erythrocytes: evidence for a conserved site-specificity in intermediate filament-membrane interactions. *Proc. Natl. Acad. Sci. USA* **84**, 6780–6784.

Granger, B. L. and Lazarides, E. (1979). Desmin and vimentin coexist at the periphery of the myofibril Z disc. *Cell* **18**, 1053–1063.

Granger, B. L. and Lazarides, E. (1982). Structural associations of synemin and vimentin filaments in avian erythrocytes revealed by immunoelectron microscopy. *Cell* **30**, 263–275.

James, R. S., Altringham, J. D. and Goldspink, D. F. (1995). The mechanical properties of fast and slow skeletal muscles of the mouse in relation to their locomotory function. *J. Exp. Biol.* **196**, 491–502.

Lazarides, E. (1980). Intermediate filaments as mechanical integrators of cellular space. *Nature* **283**, 249–256.

Lazarides, E. (1982). Intermediate filaments: a chemically heterogeneous, developmentally regulated class of proteins. *Annu. Rev. Biochem.* **51**, 219–250.

Li, Z., Colucci-Guyon, E., Picon-Raymond, M., Mericskay, M., Pourmin, S., Paulin, D. and Babinet, C. (1996). Cardiac lesions and skeletal myopathy in mice lacking desmin. *Dev. Biol.* **175**, 362–366.

Li, Z., Mericskay, M., Agbulut, O., Butler-Browne, G., Carlsson, L., Thornell, L. E., Babinet, C. and Paulin, D. (1997). Desmin is essential for the tensile strength and integrity of myofibrils but not for myogenic commitment, differentiation and fusion of skeletal muscle. *J. Cell Biol.* **139**, 129–144.

Lieber, R. L., Thornell, L.-E. and Fridén, J. (1996). Muscle cytoskeletal disruption occurs within the first 15 min of cyclic eccentric contraction. *J. Appl. Physiol.* **80**, 278–284.

Maniotis, A. J., Chen, C. S. and Ingber, D. E. (1997). Demonstration of mechanical connections between integrins, cytoskeletal filaments and nucleoplasm that stabilize nuclear structure. *Proc. Natl. Acad. Sci. USA* **94**, 849–854.

Milner, D. J., Mavroidis, M., Weisleder, N. and Capetanaki, Y. (2000). Desmin cytoskeleton linked to muscle mitochondrial distribution and respiratory function. *J. Cell Biol.* **150**, 1283–1298.

Milner, D. J., Weitzer, G., Tran, D., Bradley, A. and Capetanaki, Y. (1996). Disruption of muscle architecture and myocardial degeneration in mice lacking desmin. *J. Cell Biol.* **134**, 1255–1270.

Price, M. G. (1987). Skelemins: Cytoskeletal proteins located at the periphery of M-discs in mammalian striated muscle. *J. Cell Biol.* **104**, 1325–1336.

Price, M. G. and Gomer, R. H. (1993). Skelemins, a cytoskeletal M-disc periphery protein, contains motifs of adhesion/recognition and intermediate filament proteins. *J. Biol. Chem.* **268**, 21800–21810.

Richardson, F. L., Stromer, M. H., Huiatt, T. W. and Robson, R. M. (1981). Immunoelectron and immunofluorescence localization of desmin in mature avian muscles. *Eur. J. Cell Biol.* **26**, 91–101.

Sam, M., Shah, S., Fridén, J., Milner, D. J., Capetanaki, Y. and Lieber, R. L. (2000). Desmin knockout muscles generate lower stress and are less vulnerable to injury compared to wildtype muscles. *Am. J. Physiol.* **279**, C1116–C1122.

Tokuyasu, K. T., Dutton, A. H. and Singer, S. J. (1982). Immunoelectron microscopic studies of desmin (skeletin) localization and intermediate filament organization in chicken skeletal muscle. *Cell Biol.* **96**, 1727–1735.

Wang, K. and Ramirez-Mitchell, R. (1983). A network of transverse and longitudinal intermediate filaments is associated with sarcomeres of adult vertebrate skeletal muscle. *J. Cell Biol.* **96**, 562–570.

Weibel, E. R. (1980). Practical methods for biological morphometry. In *Stereological Methods*, pp. 28–30. New York: Academic Press.